THE JOURNAL OF BIOLOGICAL CHEMISTRY
Vol. 279, No. 30, Issue of July 23, pp. 31429–31439, 2004
Printed in U.S.A.

Identification and Activity of a Series of Azole-based Compounds with Lactate Dehydrogenase-directed Anti-malarial Activity*[S]

Received for publication, March 3, 2004, and in revised form, April 22, 2004
Published, JBC Papers in Press, April 26, 2004, DOI 10.1074/jbc.M402433200

Angus Cameron‡, Jon Read‡, Rebecca Tranter‡, Victoria J. Winter‡§, Richard B. Sessions‡, R. Leo Brady‡¶, Livia Vivas‖, Anna Easton‖, Howard Kendrick‖, Simon L. Croft‖, David Barros, Jose Luis Lavandera**, José Julio Martin**, Felix Risco**, Silvestre García-Ochoa**, Fracisco Javier Gamo**, Laura Sanz**, Luisa Leon**, Jose R. Ruiz**, Raquel Gabarró**, Araceli Mallo**, and Federico Gómez de las Heras****

*From the ‡Department of Biochemistry and Molecular Recognition Centre, University of Bristol, Bristol BS8 1TD, ‖London School of Hygiene and Tropical Medicine, Keppel Street, London WC1E 7HT, United Kingdom, and **GlaxoSmithKline, Parque Tecnológico de Madrid, Severo Ochoa, 2, 28760-Tres Cantos, Madrid, Spain*

***Plasmodium falciparum*, the causative agent of malaria, relies extensively on glycolysis coupled with homolactic fermentation during its blood-borne stages for energy production. Selective inhibitors of the parasite lactate dehydrogenase (LDH), central to NAD^+ regeneration, therefore potentially provide a route to new anti-malarial drugs directed against a novel molecular target. A series of heterocyclic, azole-based compounds are described that preferentially inhibit *P. falciparum* LDH at sub-micromolar concentrations, typically at concentrations about 100-fold lower than required for human lactate dehydrogenase inhibition. Crystal structures show these competitive inhibitors form a network of interactions with amino acids within the active site of the enzyme, stacking alongside the nicotinamide ring of the NAD^+ cofactor. These compounds display modest activity against parasitized erythrocytes, including parasite strains with known resistance to existing anti-malarials and against *Plasmodium berghei* in BALB/c mice. Initial toxicity data suggest the azole derivatives have generally low cytotoxicity, and preliminary pharmacokinetic data show favorable bioavailability and circulation times. These encouraging results suggest that further enhancement of these structures may yield candidates suitable for consideration as new therapeutics for the treatment of malaria. In combination these studies also provide strong support for the validity of targeting the *Plasmodium* glycolytic pathway and, in particular, LDH in the search for novel anti-malarials.**

Plasmodium parasites are believed to lack a functional Krebs (citric acid) cycle for at least part of their life cycle and hence rely extensively on ATP generation via the anaerobic fermentation of glucose (see Ref. 1 for review). The energy requirement of the parasitized erythrocyte is such that utilization of glucose is up to 100 times greater than in nonparasitized erythrocytes (2, 3), and virtually all glucose can be accounted for by production of lactate (2). Lactate dehydrogenase (LDH),[1] the last enzyme in the glycolytic pathway in *Plasmodium falciparum*, is a 2-hydroxy acid oxidoreductase that converts pyruvate to lactate and simultaneously the conversion of NADH to NAD^+. As a constant supply of NADH is a prerequisite for glycolysis, and LDH acts as the primary source in *Plasmodium* for the regeneration of NADH from NAD^+, inhibition of LDH is expected to stop production of ATP, with subsequent *P. falciparum* cell death. Any compound that blocks the LDH enzyme is a potentially potent antimalarial with a different mode of action to existing drugs. As such, *P. falciparum* lactate dehydrogenase (*pf*LDH) has been suggested as a drug target by several authors (4–6). One well recognized difficulty is that the drug must potently inhibit *pf*LDH yet show much less activity against the three human LDH (*hs*LDH) isoforms.

A comparison of the crystal structures of both *P. falciparum* and human LDH (7, 8) shows the following two key differences: namely positioning of the NADH factor, reflecting sequence changes in the cofactor binding pocket that displace the nicotinamide ring by about 1.2 Å, and a change in the sequence (including a 5-residue insertion) and secondary structure of a loop region that closes down on the active site during catalysis. These changes combine to produce an increase in the volume of the active site cleft in *pf*LDH relative to its human counterparts. In addition to these structural variations, there are significant kinetic differences between the two enzymes; indeed, by using the NADH derivative 3-acetylpyridine adenine dinucleotide, kinetic differences between human and *pf*LDH are so great that the observed LDH activity can be used as an indication of *in vivo* parasitemia (9). Together, the structural and kinetic discrepancies between the mammalian and malarial enzymes suggest that specific and potent *pf*LDH inhibitors can be designed or identified.

Several groups are known to have targeted *pf*LDH in drug discovery studies. Derivatives of the gossypols have been considered as *pf*LDH inhibitors. Gossypol is a polyphenolic binaphthyl disesquiterpene found in cottonseed oil, has been shown to inhibit LDHs at sub-micromolar (0.7 μM) levels (10), is compet-

* This work was in part supported by a grant from the Medicines for Malaria Venture (Geneva, Switzerland). The costs of publication of this article were defrayed in part by the payment of page charges. This article must therefore be hereby marked "*advertisement*" in accordance with 18 U.S.C. Section 1734 solely to indicate this fact.

[S] The on-line version of this article (available at http://www.jbc.org) contains additional text and Tables S1A–S1D.

The atomic coordinates and structure factors (codes 1T24, 1T25, 1T26, 1T2C, 1T2D, 1T2E, and 1T2F) have been deposited in the Protein Data Bank, Research Collaboratory for Structural Bioinformatics, Rutgers University, New Brunswick, NJ (http://www.rcsb.org/).

§ Supported by a studentship from the Biotechnology and Biological Sciences Research Council (BBSRC), United Kingdom.

¶ To whom correspondence should be addressed. Tel.: 44-117-928-7436; Fax: 44-117-928-8274; E-mail: L.Brady@bris.ac.uk.

[1] The abbreviations used are: LDH, lactate dehydrogenase; *pf*LDH, Plasmodium falciparum lactate dehydrogenase; hsLDH, human lactate dehydrogenase.

itive for NADH, and exhibits *in vitro* anti-malarial activity (4) with an IC_{50} of 10 μM. However, gossypol is cytotoxic. Attempts to derivatize gossypol have produced several compounds retaining activity against both the target enzyme and the parasite but without significantly improving selectivity or parasiticidal activity. The synthesis of derivatives of 8-deoxyhemigossylic acid has also been reported (11). This class of chemicals has been developed in an attempt to reduce the toxicity believed to be associated with the aldehyde group present in gossypol and to increase the specificity of inhibition. The hemigossypols exhibit low micromolar inhibition of LDHs and are competitive for NADH, and some of these compounds are selective inhibitors of *pf*LDH with respect to human LDH (11). One such compound, 7-*p*-trifluoromethylbenzyl-8-deoxyhemigossylic acid, has a reported K_i of 13, 81, and 4 μM, respectively, for human heart, muscle, and sperm LDH (12) and 0.2 μM for *pf*LDH (4). Vander Jagt and co-workers have also investigated various *N*-substituted hydroxamic acid derivatives and reported 35–80 μM activity *versus pf*LDH (13) and 0.3–10 mM activity *versus* human LDH (12). Modifications do not appear to affect potency significantly or the selectivity of these compounds, which appear to be competitive for pyruvate. No parasiticidal activity has been reported for these compounds.

In this paper we report the discovery of a new class of compounds that inhibit *pf*LDH and also display anti-malarial activity. Initially identified in a high throughput enzymatic assay, these compounds have been shown to interact directly and preferentially with *pf*LDH through x-ray crystallographic and steady-state kinetic analyses. They have been further characterized in parasiticidal whole-cell assays using drug-sensitive and -resistant strains of *Plasmodium*, and have been demonstrated to have *in vivo* anti-malarial activity using the *Plasmodium berghei* rodent model. In combination these results help demonstrate the viability of targeting *pf*LDH in the development of novel anti-malarials and provide examples of compounds that could be further developed to provide novel therapeutics for targeting the *Plasmodium* glycolytic pathway.

EXPERIMENTAL PROCEDURES

High Throughput Enzymatic Screen—An LDH enzymatic assay developed for high throughput format was used in a high throughput screen. The dehydrogenase reaction was run in the reverse (lactate → pyruvate) direction and coupled with the ability of diaphorase to reduce *p*-iodonitrotetrazolium violet using the NADH generated in the conversion of lactate to pyruvate (14). The progression of the coupling reaction was monitored as the increase of absorbance at 492 nm. In the initial screen, potential inhibition of both *pf*LDH and human LDH (both expressed as recombinant proteins and purified as described previously (7)) was monitored at single sample points corresponding to 25 μg/ml of the compound in 5% Me_2SO; 0.15 mM NAD^+; 1.5 mM lactic acid; 1 mM INT; 18 μg/ml Diaphorase; and 1 μg/ml *pf*LDH or human LDH. Positive hits were subjected to additional analysis to determine IC_{50} values.

Synthesis of Azole Derivatives—The parent compounds of the isooxazole and oxadiazole families were prepared in multigram scale by simple modification of the methods described in the literature (15). A range of azoles was synthesized by the introduction of substituents at the hydroxyl and acid moieties of the parent compounds (positions 3 and 4, respectively, Fig. 1). The replacement of heteroatoms within the ring structure was also considered, and the details of the modifications studied are all included in Tables I–IV. Synthetic routes for these derivatives are described in the Supplemental Material.

Crystallographic Analysis of Enzyme-Azole Inhibitory Complexes—Crystals of *pf*LDH and human LDH were grown by using either NADH or NAD^+ as cofactor as described in Refs. 8 and 7, respectively. Ligands were introduced to these crystals dissolved in the crystallization mother liquor substituted with up to 30% Me_2SO. Diffraction data were collected at the Daresbury SRS synchrotron (station PX14.1), Hamburg DESY synchrotron (station X11), or using the Nonius® FR591 rotating anode laboratory source (Nonius BV, Netherlands) and processed using the HKL suite of programs (16). Structures were solved using the phases from the isomorphous structure of the ternary complex of *pf*LDH (Protein Data Bank accession code 1LDG) or human LDH (Protein Data Bank accession code 1IOZ) and refined using the program REFMAC5 (17).

Kinetic Analysis—Although the dehydrogenase reaction was run in the reverse (lactate → pyruvate) direction for the high throughput screen, a more thorough kinetic analysis of selected inhibitors was based on the reaction run in the forward direction and monitored by measuring the change in molar absorbance of NADH at 340 nm as described previously (18). For kinetic analysis in the reverse direction, reactions containing 2 mM phenazine ethosulfate, 1 mg/ml *p*-nitrotetrazolium blue, 1 mM NAD^+, and varying concentrations of lactate in PET buffer (50 mM Tris-HCl, pH 7.5, 50 mM KCl, 1 mM EDTA, 3% (w/v) PEG 6000) were initiated by the addition of *pf*LDH to 4.4 nM and monitored by the increase in absorbance at 655 nm at 25 °C. Data were analyzed by using nonlinear least squares regression with the software package DynaFit™ (Biokin Ltd.) (19). Calculations of k_{cat} depended upon the protein concentration as measured at 280 nm by using an extinction coefficient of 1.16 mg/ml·cm for H4-*hs*LDH proteins, 1.2 mg/ml·cm for M4-*hs*LDH (20), and 0.5 mg/ml·cm for *pf*LDH. The pK_a of the active site histidine was estimated by fitting the variation of $K_{M(obs)}$ with pH to $K_{M(obs)} = K_M(1 + 10^{-pK}/10^{-pH})$ as described previously (7).

In Vitro Anti-plasmodial Activity—The drug-sensitive 3D7 clone of the NF54 isolate (21) and the chloroquine-, pyrimethamine-, and cycloguanil-resistant K1 strain (Thailand) were acquired from MR4 (Malaria Research and Reference Reagent Resource Center, Manassas, VA). *P. falciparum in vitro* culture was carried out following standard methods (22) with modifications. Briefly, parasites were maintained in tissue culture flasks in human A Rh^+ erythrocytes at 5% hematocrit in RPMI 1640 supplemented with 25 mM HEPES, 24 mM $NaHCO_3$, 0.2% (w/v) glucose, 0.03% L-glutamine, 150 μM hypoxanthine, and 0.5% Albumax II® (Invitrogen) in a 5% CO_2, 95% air mixture at 37 °C, and the medium was changed daily.

The method used to test drug susceptibility was modified from the protocol described previously (23). Briefly, stock drug solutions were dissolved in 100% Me_2SO in glass bottles, and serial dilutions of the drugs were prepared in assay medium (RPMI 1640 supplemented with 0.5% Albumax II® (Invitrogen), 0.2% w/v glucose, 0.03% L-glutamine, and 15 μM hypoxanthine), in triplicate, in 96-well plates. This was followed by the addition of 50 μl of asynchronous (65–75% ring stage) *P. falciparum* culture (0.5% parasitemia) or uninfected erythrocytes at 5% hematocrit to each well in assay medium. Plates were incubated at 37 °C, in 5% CO_2, 95% air mixture for 24 h, followed by the addition of 20 μl (0.1 μCi/well) of [^{3}H]hypoxanthine to each well. Plates were mixed for 1 min using a plate shaker and returned to the incubator. After an additional 24-h incubation period, the experiment was terminated by placing the plates in a −80 °C freezer. Plates were thawed and harvested onto glass fiber filter mats using a cell harvester (Tomtec) and dried. After the addition of Meltilex® solid scintillant (Wallac), the incorporated radioactivity was counted using a Wallac® 1450 Betalux scintillation counter (Wallac). All assays included chloroquine diphosphate as a standard and control wells with untreated infected and uninfected erythrocytes. Data acquired by the Wallac® BetaLux scintillation counter were exported into a MICROSOFT® EXCEL spreadsheet (Microsoft Corp.), and the IC_{50}/IC_{90} values of each drug were calculated by using XLFit® (ID Business Solutions Ltd., UK) line fitting software.

In Vivo Antimalarial Activity—A preliminary experiment was undertaken at a single dose to evaluate the activity of two leading compounds from the heterocyclic series. Compounds OXD1 and IOA1 (see Tables I–IV for structures) were tested in the *P. berghei* model by using the 4-day suppressive test, as indicated by Peters (24), and using chloroquine as a positive control. Briefly, naive 18–20-g BALB/C mice were infected intravenously with 2×10^6 parasitized red cells on day +0. For administration, compounds were freshly prepared in 10% Me_2SO in sterile phosphate-buffered saline the day of use. Two hours post-infection mice received the first treatment by the intraperitoneal route. Mice were further treated on days +1–3. Blood films from tail blood were prepared on day +4, and parasitemia was determined by microscopic examination of Giemsa-stained blood films. A further experiment was carried out to determine oral bioavailability and the ED_{50} value of the compounds in an *in vivo* dose-response experiment. Compounds OXD1, IOA1, and TDA1 were tested at 100, 50, 25, and 12.5 mg/kg/day by the intraperitoneal route and at 100 mg/kg/day by the oral route. Chloroquine was used as a positive control at 10 mg/kg/day by the intraperitoneal route. Mice were treated and levels of parasitemia determined as described for the single dose experiment.

Pharmacokinetic Studies—A preliminary study to assess the plasma levels of OXD1 and IOA1 was performed by intraperitoneal or oral administration of each compound to mice inoculated 2 h earlier with 1 ×

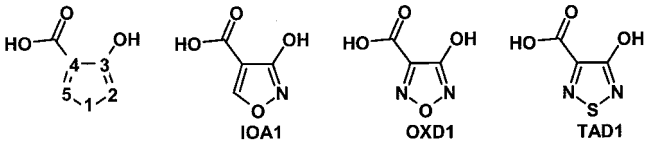

FIG. 1. **Azole-based inhibitors of pfLDH.** Schematic showing chemical structures of OXD1, IOA1, and TDA1 parent compounds.

TABLE I
Activity of 1,2,5-oxadiazole (OXD) series

N/D, not determined.

Compound	Structure	IC_{50} *pf*LDH (μM)	IC_{50} *hs*LDH (μM)	IC_{50} [IC_{90}] 3D7 (μM)	IC_{50} [IC_{90}] K1 (μM)
OXD1	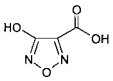	0.65	72.05	22.5 [75.9]	18.6 [143]
OXD2	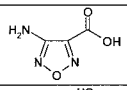	>200	>200	N/D	N/D
OXD3	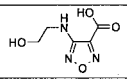	>200	>200	N/D	N/D
OXD4		>200	>200	N/D	N/D
OXD5	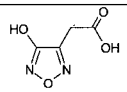	>200	>200	N/D	N/D
OXD6	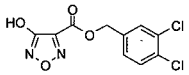	>200	>200	54.4 [> 87]	N/D
OXD7	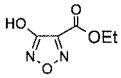	>100	>100	89.8 [>159]	N/D
OXD8	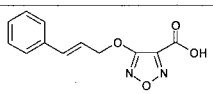	>200	>200	69.4 [>102]	N/D
OXD9	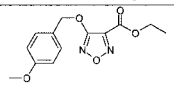	>200	>200	N/D	N/D

TABLE II
1,2/1,5-Isoxazole (IOA) series

N/D, not determined.

Compound	Structure	IC_{50} *pf*LDH (μM)	IC_{50} *hs*LDH (μM)	IC_{50} [IC_{90}] 3D7 (μM)	IC_{50} [IC_{90}] K1 (μM)
IOA1	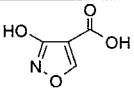	1.1	54	74.4 [>194]	N/D
IOA2	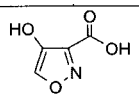	16	>100	>194 [>194]	N/D
IOA3	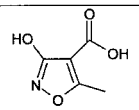	>100	>100	N/D	N/D
IOA4	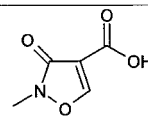	>100	>100	N/D	N/D
IOA5	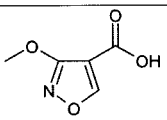	>100	>100	N/D	N/D
IOA6	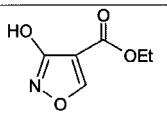	>100	>100	>59 [>159]	N/D
IOA7	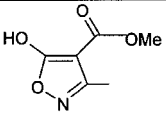	>100	>100	N/D	N/D
IOA8	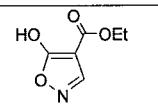	>100	>100	>59 [>159]	N/D
IOA9	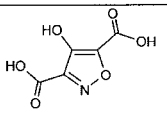	81.01	>100	N/D	N/D

10^7 *P. berghei* parasitized erythrocytes. Plasma samples were collected from three mice at each time point: 30-, 90-, and 180-min post-compound administration. Plasma concentrations of OXD1 and IOA1 were determined by peak integration after separation by using standard liquid chromatography/mass spectrometry analysis techniques.

In Vitro Cytotoxicity Assays—Cytotoxicity of OXD1 against mammalian cells was assessed by standard methods (25). Sterile 96-well microtiter plates were seeded with 100 μl of KB cells at 4×10^4/ml in RPMI 1640 supplemented with 10% heat-inactivated fetal calf serum (complete medium). Plates were incubated at 37 °C, 5% CO_2, 95% air mixture for 24 h. Compounds were dissolved in 100% Me_2SO at 20 mg/ml. For the assays, serial dilutions of the compounds were prepared in triplicate using complete medium. Culture supernatants were removed and replaced by the serial dilutions at 300, 30, 3, and 0.3 μg/ml. The positive control drug was podophyllotoxin (Sigma). Plates were incubated for a further 72 h followed by the addition of 10 μl of AlamarBlue® (AccuMed International Inc.) to each well and incubation for 2–4 h at 37 °C, 5% CO_2, 95% air mixture before reading fluorescence emission at 585 nm after excitation at 530 nm in a SPECTRAMAX® GEMINI plate reader (Molecular Devices Inc). ED_{50} values were calculated using XLFit® (ID Business Solutions Ltd., UK) line fitting software.

RESULTS

High Throughput Enzymatic Screen—Screening of over 500,000 compounds primarily from the Glaxo Wellcome proprietary chemical collection identified a number of chemical families of interest that had a *pf*LDH IC_{50} between 0.05–0.01 μg/ml and a selectivity ratio *pf*LDH/*hs*LDH IC_{50} >10. One of these families consisted of compounds that will be collectively referred to as the azoles (Fig. 1). All three parent compounds had a consistent substitution pattern with a hydroxy function and a carboxyl moiety in adjacent positions (3,4-di-substitution).

Synthesis and Activity of Azole Derivatives—A series of compounds was synthesized with the aim of exploring the structure activity relationships of the parent azoles. As shown in Tables I–IV, we tested examples of derivatives at all five positions of the pentacyclic ring, as well as heterocyclic variations within the ring structure itself. In summary, modifications to or substitution of the C-3 hydroxyl and C-4 carboxyl groups resulted in the loss of at least 2 orders of magnitude of activity against *pf*LDH, and none of the ethers, esters, or bioisosters of the hydroxyl or acid moieties were active. Modifying the heterocyclic nature of the ring by substituting the oxygen at position 1 with sulfur (resulting in the thiadiazole family, see Table III) increased the potency slightly but also led to a slight reduction in specificity. Substitution at the same position with nitrogen (leading to the triazoles, see Table IV) was nonproductive. The rationale for the wide variations in potency when modifying

TABLE III
1,2,5-Thiadiazole (TDA) series

N/D, not determined.

Compound	Structure	IC_{50} *pf*LDH (μM)	IC_{50} *hs*LDH (μM)	IC_{50} [IC_{90}] 3D7 (μM)	IC_{50} [IC_{90}] K1 (μM)
TDA1	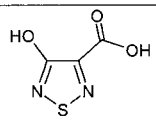	0.14	10.27	75.3 [>171]	144 [>171]
TDA2	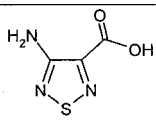	>100	>100	N/D	N/D
TDA3	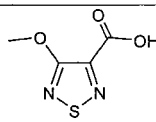	>100	>100	N/D	N/D

TABLE IV
Triazole (TRZ) series

N/D, not determined.

Compound	Structure	IC_{50} *pf*LDH (μM)	IC_{50} *hs*LDH (μM)	IC_{50} [IC_{90}] 3D7 (μM)	IC_{50} [IC_{90}] K1 (μM)
TRZ1	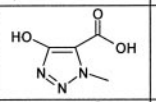	>100	>100	N/D	N/D
TRZ2	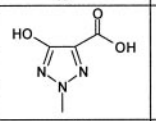	>100	>100	N/D	N/D
TRZ3	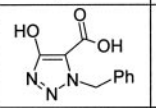	>100	>100	N/D	N/D
TRZ4	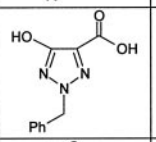	>100	>100	N/D	N/D
TRZ10	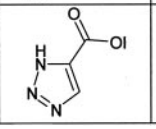	98	>200	N/D	>884 [> 221]

position 1 could be rationalized as arising from either steric hindrance (as the presence of nitrogen in position 1 introduces an extra substituent in the ring) or electronic effects (as the presence of the nitrogen modifies the pK_a of the hydroxyl group). As will be shown later, the acidity of the 2-hydroxyl group is a key factor that determines the types of interactions established by the substrate into the active site. Activity is retained if the ring nitrogens at positions 2 and 5 are substituted with carbon to produce the isooxazoles (Table II), but substitution at position 2 is less well tolerated. Despite this, the introduction of methyl groups at either of these positions reduces activity to greater than 100 μM.

Crystallographic Analysis of Enzyme-Azole Inhibitory Complexes—A summary of the diffraction data and refinement statistics for complexes of *pf*LDH with OXD1, TDA1, and IOA1 and human LDH with OXD1 is shown in Table V.

The hydroxy acid heterocyclic azole OXD1 binds in the active site of both human and plasmodial LDH, alongside the NAD^+ cofactor (Fig. 2, *a* and *b*). The carboxyl acid group of the inhibitor forms salt bridges with Arg-171 and Arg-109 of the active site loop, mimicking the interactions of the pyruvate substrate (8). The hydroxyl group of the oxadiazole contributes to a hydrogen bond network with the side chains of residues Asn-140, His-195, and Arg-109. In both the human and plasmodial crystal structures, the heterocyclic ring of the inhibitor is stacked parallel to the nicotinamide ring of the NAD^+ cofactor, whereas the nitrogen in position 2 of the heterocyclic ring is within Van der Waals radii of the NAD^+ and the side chain amine of Asn-140. In the plasmodial structure, the side of the heterocyclic ring harboring the carboxyl group is in close proximity to Pro-246 (threonine in *hs*LDH), and the Oγ of Ser-245 forms hydrogen bonds with both the ring oxygen of the inhibitor and the cofactor (via a bound water molecule). In the human LDH structure, the ring oxygen of the inhibitor is hydrogen-bonded to a water molecule, but this water appears to make no contacts with the protein itself.

The closely related inhibitors TDA1 (Table III) and IOA1 (Table II) bind in a manner virtually identical to that of OXD1, although there is small offset of <1 Å in the ring position when measured at position 1 (Fig. 3). Apart from this offset, all other features of the complex, including the surrounding protein residues, are essentially identical to those seen in the *pf*LDH: OXD1 structure. In all three complexes, the oxygen or sulfur at position 1 forms a hydrogen bond with the side chain of Ser-245. This interaction is absent in the crystal structure of OXD1 bound to human LDH, where the equivalent residue is a tyrosine but projects away from the bound inhibitor. Ser-245 and Pro-246 adopt different conformations when neither substrate nor inhibitor is bound, as seen in the crystal structure of the binary complex (Fig. 4). The adjacent "active site loop" is also disordered in this binary complex as is commonly observed for this class of oxidoreductase enzymes.

Kinetic Analysis—We used steady-state kinetics to examine the mode of binding of the azole inhibitor family. All active azoles exhibited mixed inhibition against both NADH and pyruvate and competitive inhibition against lactate (Fig. 5). Kinetically, LDH behaves as a sequential ordered bi-bi enzyme with the cofactor binding prior to substrate and being released after the product. The azoles hence bind preferentially to the enzyme-NAD^+ complex, mimicking the nonspecific inhibitor oxalate (26). The measured inhibitory constants (K_i) were 210 nM for OXD1, 470 nM for IOA1, and 290 nM for TDA1.

PfLDH Ser-245 → Ala Mutant—Crystal structures of the azoles bound to pfLDH suggested the hydrogen bond formed between the oxygen or sulfur in position 1 of the azole, and the Oγ of Ser-245 was likely to be a major determinant of selectivity for the malarial form of the enzyme. To test this hypothesis, we used site-directed mutagenesis to change the side chain at position 245 to alanine. Co-crystallization of the *pf*LDH Ser-245 → Ala mutant with oxamate (a substrate analogue) and NADH shows that the active site loop occupies the "closed" position previously seen in the wild type ternary complex, but the Ala-245 to Pro-246 region is in the "open" conformation normally seen in the binary (enzyme-cofactor) complex (Fig. 6). In the structure of the wild type enzyme co-crystallized with NADH and oxamate, the Oγ of Ser-245 forms a hydrogen bond with a water molecule that is in turn bonded to the cofactor ribose group. This water molecule is not present in the crystal structure of the mutant. The inability of the alanine side chain in the mutant to interact with the ribose group appears to correlate with the Ala-245 to Pro-246 region remaining in the open conformation, in turn probably explaining the reduced activity of this mutant enzyme (Table VI). The critical interaction formed between the serine in wild type *pf*LDH and the azole inhibitors raises the possibility that resistance to this

TABLE V
Data collection and refinement statistics

R.M.S. indicates root mean square; PDB indicates Protein Data Back.

Data collection	*pf*LDH: OXD1:NAD$^+$	*hs*LDH: OXD1:NAD$^+$	*pf*LDH: IOA1:NADH	*pf*LDH: TDA1:NADH	*pf*LDH: NADH	*pf*LDH: OXM:NADH	*Pf*LDH S245A: OXM:NADH
Xray source	Nonius FR591	Nonius FR591	SRS PX14.1	SRS PX14.1	SRS PX14.1	DESY X11	SRS PX14.1
Wavelength	1.5418	1.5418	1.488	1.488	1.488	0.9091	1.488
Resolution range (Ǎ)	30 – 1.7	30 – 3.0	30 – 1.9	30 – 1.8	30 – 2.0	25 – 1.1	20 – 1.85
No. unique reflections	33448	27214	26093	29685	21521	127177	25934
Redundancy	2.7	2.7	4.1	5.5	4.0	5.6	4.9
Completeness (%)	96 (90)	91 (80)	99.8 (99.2)	98.5 (97.1)	98.3 (99.8)	99.7 (95.6)	98.8 (96.2)
R_{sym}	0.058 (0.188)	0.166 (0.302)	0.066 (0.227)	0.064 (0.141)	0.044 (0.105)	0.072 (0.473)	0.059 (0.289)
Average I/σ(I)	18 (5.1)	6.4 (2.6)	19.5 (4.7)	28.3 (9.2)	28.5 (10.1)	22.5 (2.1)	21.3 (3.7)
Refinement							
R_{free} (%)	16.7	27.8	18.6	20.9	18.4	15.2	19.1
R_{cryst} (%)	14.3	24.0	15.2	17.4	14.3	14.3	15.6
R.M.S. bond length (Ǎ)	0.011	0.013	0.016	0.008	0.024	0.007	0.023
R.M.S. bond angle (°)	1.544	2.103	1.667	1.300	1.815	1.287	2.375
PDB Accession Code	1T24	1T2F	1T25	1T26	1T2C	1T2D	1T2E

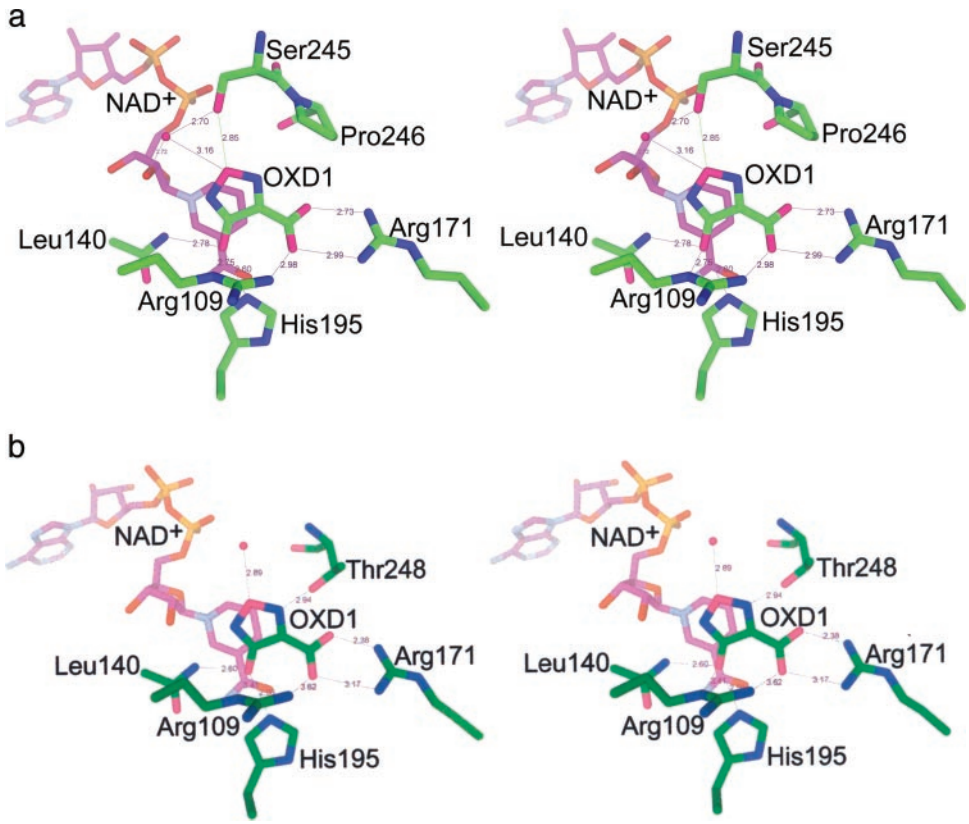

FIG. 2. **OXD1 binds in the active site of pfLDH.** Stereo figure showing the bound conformation of OXD1 in the active site of pfLDH (*a*) and human LDH (*b*). In each case the cofactor NAD$^+$ is also shown, and key amino acids are labeled. Distances of contacts between OXD1 and polar atoms from the enzyme are given in angstroms.

class of inhibitor could develop by mutating this single residue. Nonetheless, it is reassuring that the mutant enzyme produced is kinetically crippled, with a k_{cat} over 2 orders of magnitude lower than the wild type. This implies that mutation of the serine is likely to be fatal to the plasmodium. Table VI suggests the major reason for low activity in the absence of the serine is the reduced ability of the mutant enzyme to bind pyruvate ($K_{M(WT)}/K_{M(S245A)} = 114$) rather than NADH ($K_{M(WT)}/K_{M(S245A)} = 4.1$). One explanation is that the optimal binding site for the substrate may result from subtle rearrangements that follow binding of the cofactor and may involve the Ser-245 to Pro-246 region.

In Vitro Anti-plasmodial Activity—The anti-plasmodial activity of a subset of the azole series was determined against the *P. falciparum* 3D7 drug-sensitive clone and the K1 drug-resistant strain, and the measured IC_{50}/IC_{90} values are included in Tables I–IV. Only a small number of the compounds had demonstrated activity within the range of concentrations measured against whole cells, although this is likely in part to reflect the limited potency observed with the enzyme. The whole cell ac-

tivity results broadly correlated with the IC_{50} values determined against the *pf*LDH enzyme.

In Vivo Antimalarial Activity and Toxicity—In the 4-day suppressive test (24), both compounds OXD1 and IOA1 showed significant inhibition compared with untreated control mice. The percentage of inhibition observed was 41% for OXD1 and 30% for IOA1 compared with untreated controls, whereas chloroquine showed 100% inhibition. Fig. 7 illustrates the inhibitory activity observed in a dose-response experiment using the oxazoles OXD1 and IOA1 and the thiadiazole TDA1. *P. berghei* has been shown previously to contain a single gene for LDH, the product of which is kinetically and structurally virtually identical to *pf*LDH (18).

Pharmacokinetic Studies of OXD1 and IOA1—Plasma concentration time curves (area under curve plots) are shown for OXD1 and IOA1 in Fig. 8. After a single intravenous dose of 5 mg/kg, the pharmacokinetic parameters evaluated for each compound were similar. For IOA1 and OXD1, both the AUC_{0-8} and elimination half-life ($t_{1/2}$) were 4.8 and 4.6 μg·h/ml and 0.38 and 0.39 h, respectively.

Absorption of IOA1 and OXD1 after intraperitoneal administration of 20 mg/kg was very rapid, with peak plasma levels of 15.3 and 14.6 μg/ml, respectively, reached within 25 min. However, the $t_{1/2}$ of intraperitoneal administration of IOA1 (0.56 h) was approximately three times lower than that of OXD1 (1.46 h).

The time courses of drug levels in plasma for OXD1, IOA1, and TDA1 in mice after intraperitoneal or oral administration (dose, 100 mg/kg) are shown in Table VII. All compounds tested (OXD1, IOA1, and TDA1) showed consistently high plasma levels after oral administration with peak levels of 17.9, 19.8, and 35.2 μg/ml, respectively, measured 30 min post-administration. Plasma peak levels obtained after intraperitoneal administration of OXD1, IOA1, and TDA1 (25.5, 20.4, and 41.0 μg/ml, respectively) were similar to results obtained after oral administration.

In Vitro Cytotoxicity Assays—No overt toxicity was associated with OXD1 when tested against the mammalian KB (ED_{50} = 0.64 mM) and HeLa (ED_{50} = 1.3 mM) cell lines.

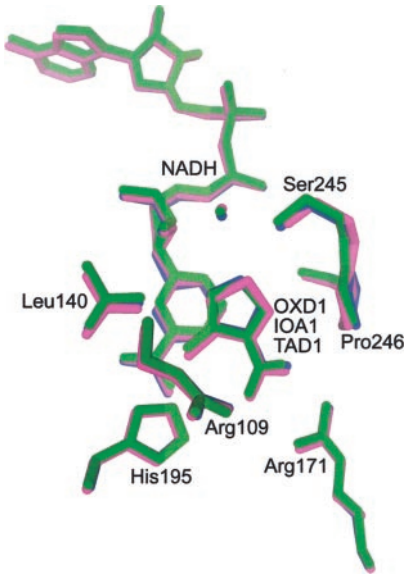

FIG. 3. **Azole-based inhibitors at the active site of *pf*LDH.** Figure shows the active site region in the crystal structures of *pf*LDH co-crystallized with NAD^+ and OXD1 (*green*), NADH and IOA1 (*blue*), and NADH with TDA1 (*magenta*).

DISCUSSION

Following early reports of enhanced rates of glycolytic turnover in *Plasmodium*-infected erythrocytes, and biochemical data suggesting the absence of a complete citric acid cycle in at least the blood-borne stages of the parasite life cycle, it was recognized that homolactic fermentation (the conversion of pyruvate to lactate with concomitant reduction of NAD+) plays a special role in survival of the malarial parasite. Although sequence (27) and structural (7, 8, 18) differences have been noted between the plasmodial and human forms of the enzymes that support the theoretical viability of targeting *pf*LDH for anti-malarial activity, there have been only a very limited number of compounds reported as specific inhibitors of this enzyme (4, 10, 11, 13, 28), and none are readily amenable to simple synthesis or free from toxicological problems. The azoles described in this paper form the first example of compounds that are readily synthetically accessible, form specific inhibitors of *pf*LDH, and have good drug-like properties.

Each of the three parent compounds (the oxadiazole OXD1, the isoxazole IAO1, and the thiadiazole TDA1) were initially discovered through an enzyme assay-based high throughput screen and inhibit *pf*LDH with low or sub-micromolar IC_{50} values, in contrast to the ~50 μM IC_{50} values observed with human LDH. The data presented in this paper provide a detailed and consistent description of the interaction of these compounds with their enzyme target.

The molecular basis of this inhibition is illustrated by the crystal structures of the enzyme-inhibitor complexes. In each case, the azole inhibitor binds directly within the active site of the enzyme, effecting closure of the active site loop that normally makes direct interactions with the keto acid (pyruvate) substrate. The concerted interactions of the substrate with this loop and its subsequent closure have been shown previously

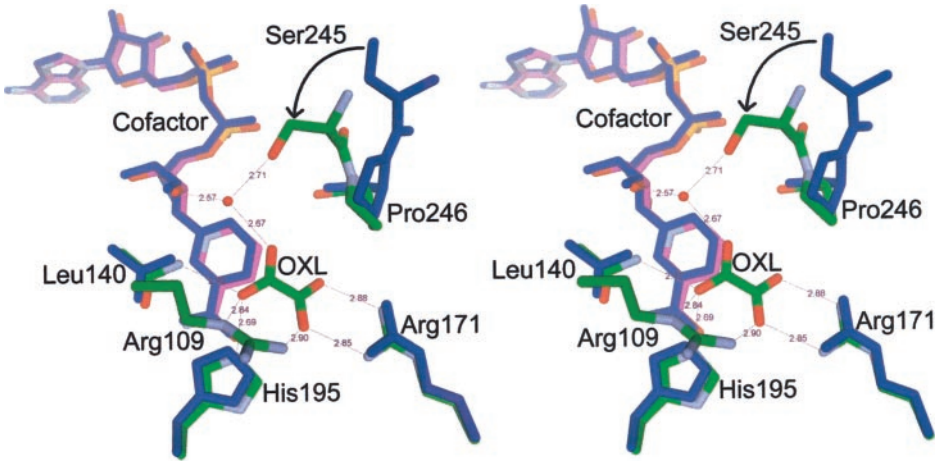

FIG. 4. **Movement of Ser-245/Pro-246 between binary and ternary complexes of *pf*LDH.** Figure shows a stereoview of the crystal structure of the *pf*LDH-NADH binary complex (*blue carbons*) overlaid on the *pf*LDH-NAD^+-oxalate ternary complex (*green carbons* except NADH carbons which are shown in *magenta*). Note that Arg-109 and the water molecule are both disordered in the binary structure, a consequence of the active site loop (residues 102–109) not being ordered in the absence of substrate. The *arrow* indicates the direction of movement of the Ser-245/Pro-246 during the transition from the binary to the ternary structure. Distances of key contacts are given in angstroms for the ternary structure.

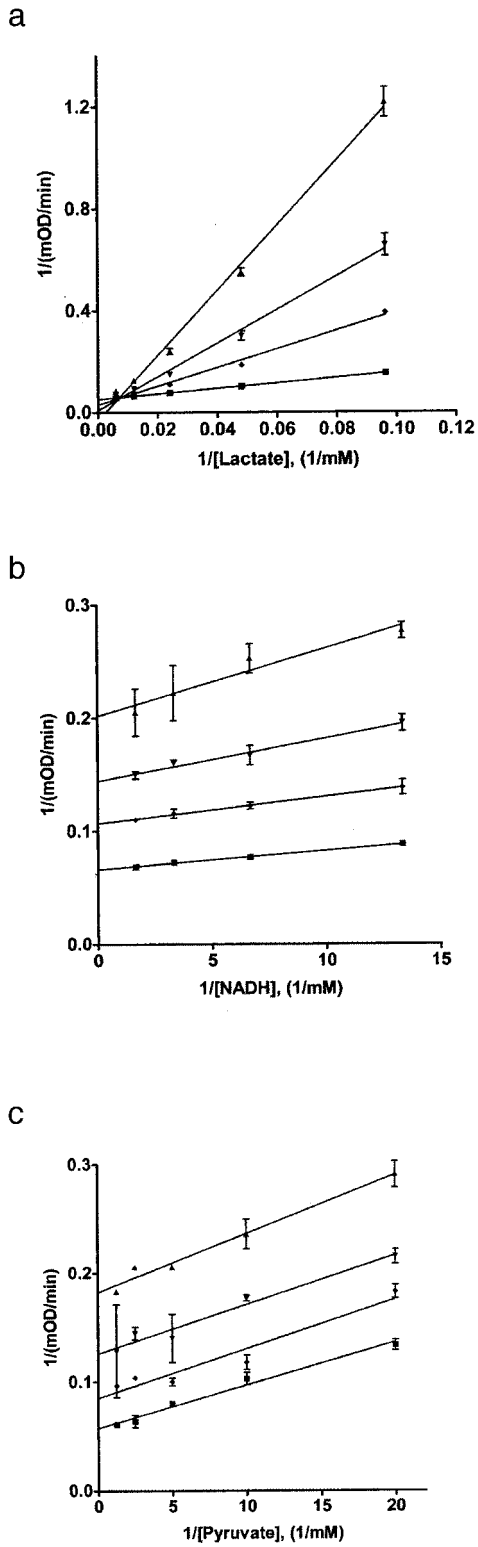

FIG. 5. **OXD1 competes with lactate for binding to *pf*LDH.** Figure shows Lineweaver-Burk plots (1/*V versus* 1/[S]) for inhibition of *pf*LDH activity when titrated against varied amounts of lactate (OXD1 concentrations at 1.0 μM (▲), 0.5 μM (▼), 0.25 μM (◆), and 0 μM (■)) (*a*), NADH (OXD1 concentrations at 12.5 μM (▲), 6.25 μM (▼), 3.125 μM (◆), and 0 μM (■)), (*b*) and pyruvate (OXD1 concentrations at 10.0 μM (▲), 5.0 μM (▼), 2.5 μM (◆), and 0 μM (■)) (*c*). The inhibition is classic competitive against lactate and mixed against NADH and pyruvate.

(29) to be a key factor in the exquisite selectivity of the lactate and, particularly, malate dehydrogenase enzymes. Replication of this complementarity with both the open and closed form of the enzyme provides a powerful means of generating inhibitor selectivity. Nonetheless, although the moderate level of activity of these compounds is encouraging, higher potency needs to be achieved to use these compounds as therapeutics. The relatively small size (M_r ~140) of the azoles suggests there is plenty of scope to enlarge these structures to enhance their contacts with the enzyme and hence increase the affinity of binding. However, their almost complete burial within the closed active site makes this problematic.

From the crystal structures a number of common interactions can be identified. The carboxylic acid group of each inhibitor forms a bifurcated salt bridge with Arg-171 and Arg-109, mimicking the interaction with the pyruvate substrate as documented previously (8) from ternary complexes of *pf*LDH with oxamate, a substrate analogue. The hydroxyl group of each azole forms a common set of hydrogen bonds with Leu-140, His-195, and Arg-109. Taken together these interactions explain why the hydroxyl-carboxyl motif is vital for the activity of these inhibitors, and why extending the inhibitor from the carboxyl or hydroxyl groups consistently results in a reduction or complete loss of activity (Tables I–IV). These interactions also support the proposition that for activity both the acid and hydroxyl groups must have suitable pK_a values to leave these groups ionized *in vivo*.

The heterocyclic ring of each inhibitor stacks parallel to the nicotinamide ring of the NAD^+ cofactor, separated by about 2 Å where π-π cloud stacking interactions would contribute to ligand binding. Similar interactions have also been noted in crystal structures of other anti-microbials active against plasmodial NAD(P)H-dependent enzymes, such as the NADPH-dependent dihydrofolate reductase (30), and Triclosan binding to the parasite NADH-dependent enoyl acyl-carrier protein reductase (31). Pro-246 lies adjacent to the carboxylate function of the heterocyclic ring, leaving little space to extend these inhibitors from the nitrogen in position 5 of the ring. This is consistent with the decrease in activity associated with the introduction of substituents at this position (Tables I–IV). Even the introduction of a simple methyl group at position 5, which the structures suggest might profitably make van der Waals contacts with the proline, is not tolerated (IOA3, Table II). The nitrogen in position 2 of the heterocyclic ring is already within Van der Waals radii of the NAD^+ and Asn-126; and extending the inhibitor in this direction is unlikely to result in tighter binding. Hence, from the crystal structures, extending the ring from position 1 is seen as the modification most likely to result in new interactions.

Importance of Ser-245—In the oxadiazole structures, the oxygen at position 1 forms a hydrogen bond with the side chain of Ser-245 (Fig. 2*a*). This interaction is likely to account for much of the selectivity of these compounds for the malarial rather than human forms of LDH, as in the latter this serine is absent, replaced by a tyrosine that is oriented away from the active site (Fig. 2*b*). Extending the azole moiety from this position would require movement of the serine side chain from its current "in" position. We noted that this was indeed possible, as in the crystal structure of the binary complex (enzyme + cofactor, Fig. 4), where the active site loop is disordered, the Ser-245/Pro-246 main chain segment adopts a more open conformation that we termed the "out" position. With the serine in this conformation, it appears there is plenty of scope to extend the azole inhibitors from the 1-position of the ring to increase contacts with residues distal from serine 245. However, as mentioned above, binding of the azole inhibitors is characterized by the formation of hydrogen bonds between arginines 109 and 171 from the enzyme with the carboxyl and hydroxy groups seen as essential for this class of inhibitor. As arginine 109 is

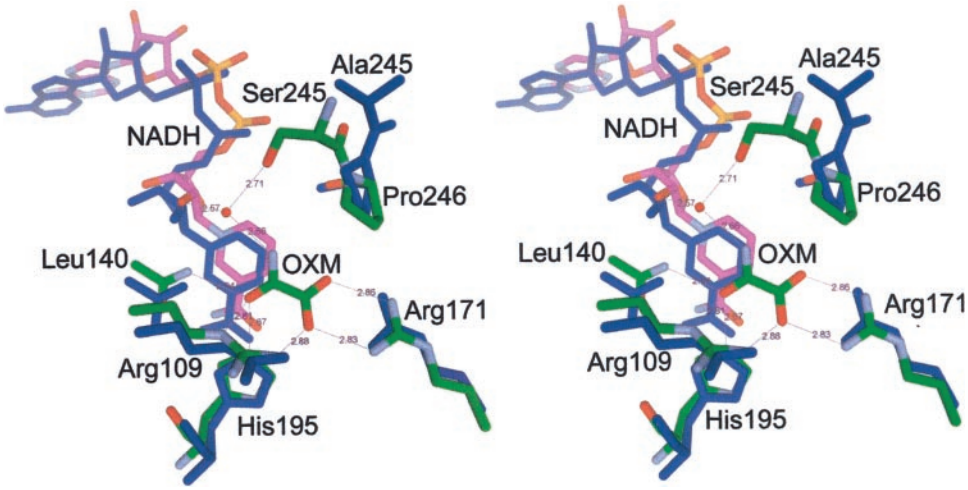

FIG. 6. **Crystal structure of the Ser-245 → Ala mutant.** Figure shows a stereoview of the active site region from the crystal structure of the Ser-245 → Ala mutant *pf*LDH (*cyan carbons*) co-crystallized with NADH and oxamate, overlaid on the structure of the wild type enzyme (*green carbons* except NADH carbons which are shown in *magenta*) co-crystallized with the same ligands. The structures are overlaid on oxamate. Note that the substrate analogue oxamate has an amide nitrogen in place of a methyl group in the natural substrate, pyruvate. Distances between polar neighbors are given in angstroms for the wild type enzyme.

TABLE VI
Kinetic properties of pfLDH Ser245 → Ala

	S245A *pf*LDH	Wild type *pf*LDH[a]
K_M NADH (μM)	66 (±2.7)	16 (±1)
K_M pyruvate (μM)	5566 (±185)	49 (±6)
K_{cat} (s^{-1})	0.42 (±0.01)	94 (±3)

[a] Data from Ref. 18.

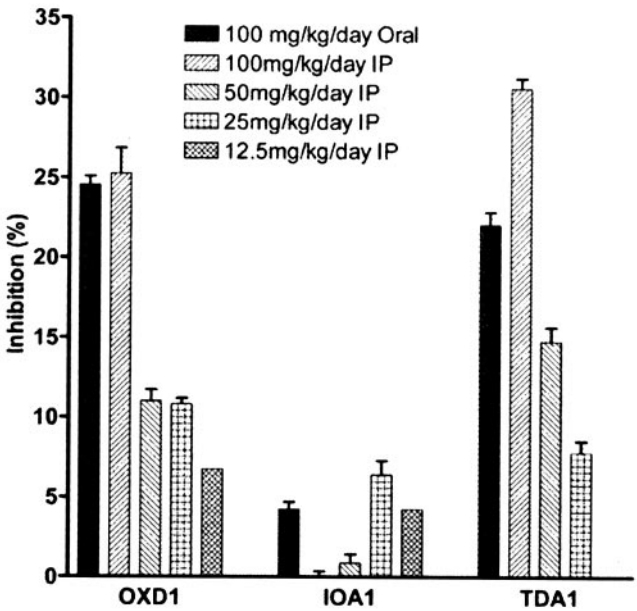

FIG. 7. ***In vivo* dose response of *P. berghei*-infected mice treated with azole-based inhibitors.** *Chart* shows the percentage inhibition of *P. berghei* in mice when treated with azole-based inhibitors administered orally (*solid bars*) and via intraperitoneal (*IP*) injection (*all other bars*). Chloroquine treatment at 10 mg/kg/day was included as a control and resulted in complete inhibition (data not shown).

part of the active site loop, the loop must therefore be closed for these bonds to be formed. We observed that in most structures of ternary or inhibitor complexes of *pf*LDH, closure of the active site loop was accompanied by movement of the Ser-245 to Pro-246 loop to the in position. To probe whether this apparently concerted movement was essential for, or subsidiary to, active site loop closure, we prepared a mutant form of *pf*LDH with Ser-245 changed to alanine.

We assessed the kinetics and crystal structure (in the presence of NADH and oxamate) of this mutant (S245A) form of *pf*LDH. As expected, the only significant differences seen between the mutant and wild type structures are in the immediate region of the Ser-245 → Ala mutation. The 245–246 loop region is in the out position, in an identical conformation to the wild type binary complex, although unlike the binary structure the active site loop of the mutant is closed. This indicates that azole binding need not necessarily require closure of Ser-245 to the in position. The loss of the hydrogen bonding capability of Ser-245 leaves the Cα atom of the mutant Ala-245 ~3 Å distant from the equivalent Cα in the wild type ternary structure, leaving plenty of scope for inclusion of 1-position substituents in the azole ring.

Intriguingly, the kinetic data show that whereas the binding affinity of the S245A mutant for NADH is decreased by only a factor of 3, the ability to bind pyruvate is much more severely reduced (a 114-fold increase in K_m for pyruvate, see Table VI). The Oγ of serine 245 in the wild type ternary structure hydrogen bonds indirectly via a water molecule to the ribose of NADH so it might be anticipated that NADH binding would be affected more by the serine to alanine mutation. However, this type of behavior has been observed in mammalian S163L LDH mutants (32, 33) where a hydrogen bond between Ser-163 and the nicotinamide amide group is removed. The conclusion of that study suggests that the hydrogen bond was more important for orienting the nicotinamide head group than for contributing to binding. The NADH binds before pyruvate in the bi-bi reaction mechanism and, in turn, forms part of the pyruvate-binding site such that misalignment of the nicotinamide-ribose group of NADH in the active site will compromise pyruvate binding. Unlike the mammalian S163L LDH mutants, the *pf*-LDH S245A mutant also shows a greatly reduced k_{cat} (224-fold). This indicates that the hydride transfer step in the *E*S complex is compromised, perhaps by misalignment of the pyruvate, whereas the 245–264 is in its open conformation.

These studies show that serine 245, absent in human LDH, is critical for the correct functioning of the *pf*LDH enzyme because of its role in the creation of the pyruvate-binding site, and to a lesser extent in the binding of NADH in the active site. Designing an antimalarial compound that interacts with this residue may therefore reduce the likelihood of viable resistant

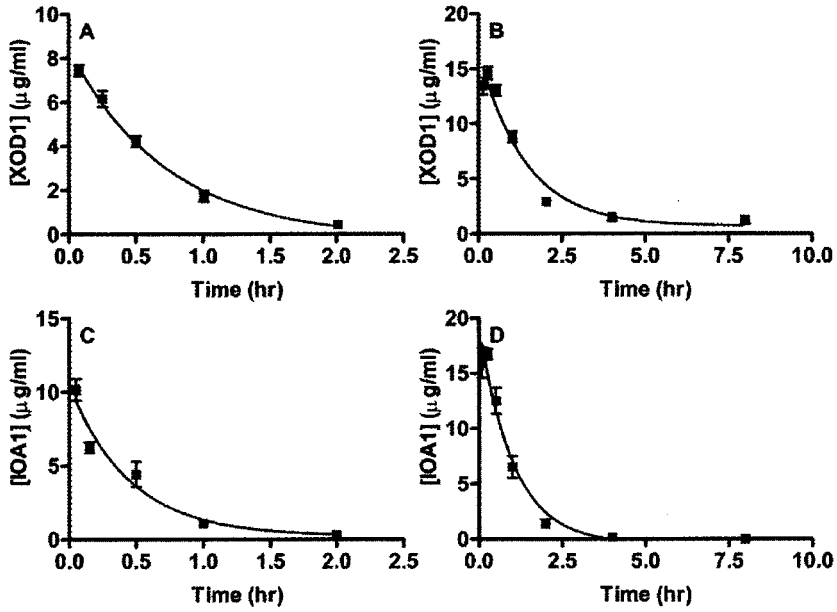

FIG. 8. **Pharmacokinetic data for azole-based inhibitors.** *Graphs* show plasma concentration time curves (AUC) for OXD1 and IOA1. Circulating levels of each compound were determined at time intervals after 5 mg/kg intravenous injection of OXD1 (*A*), 20 mg/kg intraperitoneal injection of OXD1 (*B*), 5 mg/kg intravenous injection of IOA1 (*C*), and intraperitoneal injection of IOA1 (*D*). AUC_{0-8} and elimination half-lives ($t_{1/2}$) were calculated from each curve. Data shown are fitted to a one-phase exponential decay for display purposes.

TABLE VII
Time course of drug levels in serum for OXD1, IOA1, and TDA1

Data represent the mean ± S.D. for n = 3 mice/time point.

Dose	Time	Mean serum concentration ± S.D.		
		OXD1	IOA1	TDA1
	h		*μg/ml*	
100 mg/kg p.o.[a]	0.5	17.89 ± 2.18	19.84 ± 0.81	35.19 ± 2.35
	1.5	4.77 ± 0.29	9.12 ± 1.34	19.82 ± 3.54
	3.0	4.40 ± 0.22	4.90 ± 0.77	16.09 ± 0.74
100 mg/kg i.p.[b]	0.5	25.48 ± 0.63	20.41 ± 2.46	41.03 ± 2.74
	1.5	11.99 ± 1.60	7.35 ± 2.02	26.6 ± 4.57
	3.0	2.64 ± 0.52	1.15 ± 0.30	7.56 ± 0.68

[a] p.o., post-orally.
[b] i.p., intraperitoneally.

strains of the parasite being formed, because mutation of Ser-245 severely reduces the catalytic ability of the enzyme. The structural data supported the notion that, in principle, the azole ring could be extended from the 1-position by moving Ser-245 to the out position, while still maintaining interactions of the hydroxyl and carboxyl functions of the ring with residues from an enzyme closed active site loop.

Azoles Bind as the Dianion—A limitation in the expansion of the azoles from the 1-position arises, however, from the delocalized electronic character of these pentacyclic rings along with potential keto-enolization of the 3-hydroxyl substituent. Kinetic analysis (Fig. 6) shows that OXD1 is essentially uncompetitive with pyruvate, *i.e.* it does not compete with pyruvate for the *pf*LDH-NADH pyruvate-binding site. Binding to pfLDH-NAD^+ is instead preferred by about 3 orders of magnitude (*i.e.* OXD1 is competitive with lactate), a result consistent with the crystallographic studies in which we observed significantly increased resolution of diffraction and order within the binding site when using complexes with NAD^+ rather than NADH (data not shown).

This strongly indicates that OXD1 binds as the dianion, which is consistent with the pK_a of its hydroxyl group (estimated, from chromatography studies, to be ~5), and is analogous to the behavior of oxalate. It has been noted previously (29, 34) that LDH only forms stable ternary complexes when the charges on the active site histidine, the substrate, and the coenzyme nicotinamide ring sum to 0. This requirement is satisfied if OXD1 is dianionic and His-195 is protonated, as NAD^+ is the preferred form of the cofactor. The pK_a of the active site histidine was estimated to be 8.1 ± 0.2, close to that of the human LDHs (7). Observed bond lengths in the high resolution (1.1 Å) OXD1-NAD^+-*pf*LDH complex support this arrangement, with the length of the bond between His-195 and the oxadiazole 3-hydroxy group being 2.6 Å, consistent with a charged hydrogen bond between a protonated histidine and anionic hydroxyl. The requirement for the pK_a of the azole hydroxyl group to be close to or below physiological pH considerably restrains the design of the other 5-membered ring heterocyclic compounds that might be derivatized at position 1. One explanation for the lack of inhibitory activity associated with the triazole series (Table IV) is that the pK_a of the hydroxyl group in these compounds is expected to be very high (>9.5). On this basis, synthesis of thiazoles might offer a better route forward to derivatization of this family of compounds.

Anti-malarial Activity of the Azoles—The activity of the azole series against *pf*LDH is largely paralleled in their activity against *P. falciparum*-infected erythrocytes, in both chloroquine-resistant and chloroquine-sensitive strains (Tables I–IV). All compounds that were inactive against the target enzyme also failed to kill the parasite *in vitro*; similarly, the relative activity (as reflected by the IC_{50} values) of the small number of *pf*LDH inhibitors is preserved in the whole-cell assays. Nonetheless, these are low levels of activity. This is particularly evident from the concentrations required to kill 90% of infected cells (IC_{90} values), which are considerably greater than the equivalent IC_{50} values in all cases for which the data are available. For OXD1, for example, a concentration of about 75 μM was needed to kill 90% of infected cells. This is

a lower level of activity than would normally be considered appropriate for a drug candidate.

This low level of cellular activity undoubtedly arises in part from the modest levels of activity against the target enzyme. OXD1, for example, has an IC_{50} value of just under 1 μM in the pfLDH enzymatic assay, whereas typical drug candidates show low nanomolar activity in equivalent assays. It is therefore not surprising that, for most of the compounds studied, complete killing of infected parasites could not be achieved within the normal concentrations (25 μg/ml) used for the *in vitro Plasmodium* assays. Drug uptake is an issue of particular concern with highly charged anionic compounds, such as the azoles described in this study, and is especially critical for anti-malarials where there is a need to cross at least three membranes (erythrocyte, parasitophorous vacuole, and parasite) before parasite targets can be reached. In preliminary drug uptake studies, we have found no evidence for preferential uptake of OXD1 within either infected or uninfected erythrocytes, in contrast to chloroquine controls (data not shown). This is consistent with only low levels of the OXD1 compound penetrating the cells, hence contributing to the low levels of cellular activity, or the compound is actively being extruded by an unknown transporter. There was no evidence that compounds in which the carboxylate function was esterified, hence reducing its anionic character, were more active in the whole cell (*e.g.* OXD6, OXD7, and OXD9). However, as the esters are inactive against the *pf*LDH enzyme (Table I), they would need to be hydrolyzed within the cells, a reaction that has proven difficult in our experience. Further uptake studies are required if this family of pfLDH inhibitors is to be developed.

P. berghei, frequently used as an animal model for human malaria, shares a highly homologous form of LDH (97% identical to *pf*LDH) for which the crystal structure has been determined recently (18). As the special features of the active site that distinguish *pf*LDH from its human counterparts are completely preserved in *P. berghei* LDH, it is anticipated that compounds active against *pf*LDH would also be effective against the *P. berghei* parasite. This indeed proved to be the case. In the Peters (24) 4-day test, both compounds showed significant anti-malarial activity in *P. berghei*-infected mice when compared with untreated control mice. The percentage of inhibition observed was 41% for OXD1 and 30% for IOA1 compared with untreated controls, whereas chloroquine showed 100% inhibition. The lower *in vivo* inhibitory activity of compound IOA1 compared with OXD1 correlated with their relative anti-plasmodial activity observed *in vitro* and their ability to inhibit *pf*LDH in the enzymatic assays. This trend is also seen when the inhibitory activity was measured in a dose-response experiment (Fig. 7) where both OXD1 and TDA1 both proved more effective at killing the parasite than the isoxazole IOA1. However, all three azoles were less effective than the chloroquine control. This is consistent with the moderate inhibitory levels of activity measured for the azoles against their enzyme target.

From the preliminary pharmacokinetic studies, it is clear that these three compounds showed good plasma levels but short half-lives in the circulation (see under "Pharmacokinetic Studies"). This may also contribute to the lack of complete suppression of parasitemia at doses of 50 or 100 mg/kg/day either by the oral or intraperitoneal routes. However, the good dose response observed with TDA1 and partly with OXD1 supports the notion that these compounds have specific anti-plasmodial activity. Although the solubility of IOA1 in aqueous solutions for oral dosing was poor compared with the other two compounds, despite reasonable plasma levels its anti-malarial activity showed an erratic dose response. These results show that despite these compounds exhibiting only moderate *pf*LDH activity *in vitro* and in the absence of preferential uptake to infected cells, suppression of parasitemia *in vivo* is nevertheless possible.

The unusual route for energy (ATP) generation in *Plasmodium* relative to its human host suggests targeting of glycolytic enzymes should prove a valuable source of compounds with anti-parasitic activity. This demonstration that inhibition of *pf*LDH is fatal to the parasite supports the view that, despite the recent identification of all the genes necessary for a complete tricarboxylic acid cycle in *P. falciparum* (35), an effective respiratory chain is unlikely to be functional in at least the blood-borne stages of the parasite life cycle. Although previous workers have described gossypol-like compounds that inhibit *pf*LDH, these molecules have been difficult (expensive) to synthesize and many are likely to have poor cytotoxicity profiles. In this paper we have described a new class of compounds that specifically inhibit *pf*LDH and also display anti-malarial activity. X-ray crystallographic analyses illustrate these compounds interact directly and preferentially with *pf*LDH. They have been characterized further in parasiticidal whole-cell assays using drug-sensitive and -resistant strains of *Plasmodium* and demonstrated to have modest *in vivo* anti-malarial activity using the *P. berghei* rodent model. In combination, we believe these results make a substantial case for the validation of pfLDH as a viable target for anti-malarials. Although the azoles are limited in opportunities for further derivatization because of their intimate contacts made within the active site of the enzyme, and appear to have limited cellular uptake in their current form, further development of extended azole-like compounds might prove a profitable route for the development of novel anti-malarials.

Finally, this study also demonstrates the feasibility of developing specific inhibitors against microbial targets that have direct human homologues. Small structural differences between *pf*LDH and human LDH allow sufficient discrimination for preferential inhibition of the parasite enzyme. This principle vastly increases the pool of proteins that could be used as viable drug targets.

Acknowledgment—We are grateful to the staff at the Daresbury SRS and Hamburg DESY synchrotrons for access to x-ray facilities used for this study.

REFERENCES

1. Lang-Unnasch, N., and Murphy, A. D. (1998) *Annu. Rev. Microbiol.* **52,** 561–590
2. Scheibel, L. W., Adler, A., and Trager, W. (1979) *Proc. Natl. Acad. Sci. U. S. A.* **76,** 5303–5307
3. Roth, E. F., Jr., Raventos-Suarez, C., Perkins, M., and Nagel, R. L. (1982) *Biochem. Biophys. Res. Commun.* **109,** 355–362
4. Gomez, M. S., Piper, R. C., Hunsaker, L. A., Royer, R. E., Deck, L. M., Makler, M. T., and Vander Jagt, D. L. (1997) *Mol. Biochem. Parasitol.* **90,** 235–246
5. Menting, J. G., Tilley, L., Deady, L. W., Ng, K., Simpson, R. J., Cowman, A. F., and Foley, M. (1997) *Mol. Biochem. Parasitol.* **88,** 215–224
6. Ridley, R. G. (1997) *Exp. Parasitol.* **87,** 293–304
7. Read, J. A., Winter, V. J., Eszes, C. M., Sessions, R. B., and Brady, R. L. (2001) *Proteins* **43,** 175–185
8. Dunn, C. R., Banfield, M. J., Barker, J. J., Higham, C. W., Moreton, K. M., Turgut-Balik, D., Brady, R. L., and Holbrook, J. J. (1996) *Nat. Struct. Biol.* **3,** 912–915
9. Makler, M. T., Ries, J. M., Williams, J. A., Bancroft, J. E., Piper, R. C., Gibbins, B. L., and Hinrichs, D. J. (1993) *Am. J. Trop. Med. Hyg.* **48,** 739–741
10. Royer, R. E., Deck, L. M., Campos, N. M., Hunsaker, L. A., and Vander Jagt, D. L. (1986) *J. Med. Chem.* **29,** 1799–1801
11. Deck, L. M., Royer, R. E., Chamblee, B. B., Hernandez, V. M., Malone, R. R., Torres, J. E., Hunsaker, L. A., Piper, R. C., Makler, M. T., and Vander Jagt, D. L. (1998) *J. Med. Chem.* **41,** 3879–3887
12. Yu, Y., Deck, J. A., Hunsaker, L. A., Deck, L. M., Royer, R. E., Goldberg, E., and Vander Jagt, D. L. (2001) *Biochem. Pharmacol.* **62,** 81–89
13. Dando, C., Schroeder, E. R., Hunsaker, L. A., Deck, L. M., Royer, R. E., Zhou, X., Parmley, S. F., and Vander Jagt, D. L. (2001) *Mol. Biochem. Parasitol.* **118,** 23–32
14. Allain, C. C., Henson, C. P., Nadel, M. K., and Knoblesdorff, A. J. (1973) *Clin. Chem.* **19,** 223–227
15. Wieland, H., Kitasato, Z., and Utzino, S. (1930) *Liebigs Ann. Chem.* **478,** 43–54
16. Otwinowski, Z., and Minor, W. (1997) in *Macromolecular Crystallography*

(Carter, J., C. W., and Sweet, R. M., eds) Part A, Vol. 276, pp. 307–326, Academic Press, New York
17. Collaborative Computational Project (1994) *Acta Crystallogr. Sect. D. Biol. Crystallogr.* **50,** 760–763
18. Winter, V. J., Cameron, A., Tranter, R., Sessions, R. B., and Brady, R. L. (2004) *Mol. Biochem. Parasitol.* **131,** 1–10
19. Kuzmic, P. (1996) *Anal. Biochem.* **237,** 260–273
20. Barstow, D. A., Black, G. W., Sharman, A. F., Scawen, M. D., Atkinson, T., Li, S. S., Chia, W. N., Clarke, A. R., and Holbrook, J. J. (1990) *Biochim. Biophys. Acta* **1087,** 73–79
21. Ponnudurai, T., Leeuwenberg, A. D., and Meuwissen, J. H. (1981) *Trop. Geogr. Med.* **33,** 50–54
22. Trager, W., and Jensen, J. B. (1976) *Science* **193,** 673–675
23. Desjardins, R. E., Canfield, C. J., Haynes, J. D., and Chulay, J. D. (1979) *Antimicrob. Agents Chemother.* **16,** 710–718
24. Peters, W. (1975) *Ann. Trop. Med. Parasitol.* **69,** 155–171
25. Palomino, J. C., and Portaels, F. (1999) *Eur. J. Clin. Microbiol. Infect. Dis.* **18,** 380–383
26. Novoa, W. B., Winer, A. D., Glaid, A. J., and Schwert, G. W. (1959) *J. Biol. Chem.* **234,** 1143–1148
27. Sessions, R. B., Dewar, V., Clarke, A. R., and Holbrook, J. J. (1997) *Protein Eng.* **10,** 301–306
28. Vander Jagt, D. L., Caughey, W. S., Campos, N. M., Hunsaker, L. A., and Zanner, M. A. (1989) *Prog. Clin. Biol. Res.* **313,** 105–118
29. Chapman, A. D., Cortes, A., Dafforn, T. R., Clarke, A. R., and Brady, R. L. (1999) *J. Mol. Biol.* **285,** 703–712
30. Yuvaniyama, J., Chitnumsub, P., Kamchonwongpaisan, S., Vanichtanankul, J., Sirawaraporn, W., Taylor, P., Walkinshaw, M. D., and Yuthavong, Y. (2003) *Nat. Struct. Biol.* **10,** 357–365
31. Perozzo, R., Kuo, M., Sidhu, A. B. S., Valiyaveettil, J. T., Bittman, R., Jacobs, W. R., Fidock, D. A., and Sacchettini, J. C. (2002) *J. Biol. Chem.* **277,** 13106–13114
32. Hewitt, C. O., Eszes, C. M., Sessions, R. B., Moreton, K. M., Dafforn, T. R., Takei, J., Dempsey, C. E., Clarke, A. R., and Holbrook, J. J. (1999) *Protein Eng.* **12,** 491–496
33. Eszes, C. M., Sessions, R. B., Clarke, A. R., Moreton, K. M., and Holbrook, J. J. (1996) *FEBS Lett.* **399,** 193–197
34. Wilks, H. M., Hart, K. W., Feeney, R., Dunn, C. R., Muirhead, H., Chia, W. N., Barstow, D. A., Atkinson, T., Clarke, A. R., and Holbrook, J. J. (1988) *Science* **242,** 1541–1544
35. Gardner, M. J., Hall, N., Fung, E., White, O., Berriman, M., Hyman, R. W., Carlton, J. M., Pain, A., Nelson, K. E., Bowman, S., Paulsen, I. T., James, K., Eisen, J. A., Rutherford, K., Salzberg, S. L., Craig, A., Kyes, S., Chan, M. S., Nene, V., Shallom, S. J., Suh, B., Peterson, J., Angiuoli, S., Pertea, M., Allen, J., Selengut, J., Haft, D., Mather, M. W., Vaidya, A. B., Martin, D. M., Fairlamb, A. H., Fraunholz, M. J., Roos, D. S., Ralph, S. A., McFadden, G. I., Cummings, L. M., Subramanian, G. M., Mungall, C., Venter, J. C., Carucci, D. J., Hoffman, S. L., Newbold, C., Davis, R. W., Fraser, C. M., and Barrell, B. (2002) *Nature* **419,** 498–511